Impact of window opening percentage and window opening floor height on ventilation of enclosed buildings

Ziqian Ma[1], Heng Shen[1,*], Jinqing Wan[1], Wanxvan Yu[2], Ke Zhong[2]

[1.] Department of Refrigeration and Air Conditioning, Shanghai Ocean University, Shanghai 201306, China
[2.] College of Environmental Science and Engineering, Donghua University, Shanghai 201620, China

*E-mail:shenheng86028@126.com

Abstract. To investigate the impact of opening factors on the ventilation of enclosed buildings, numerical simulations were conducted to analyze the coupling airflow between upwind and downwind buildings. The study focused on the effects of window opening percentages (5%, 7.5%, 10%, 12.5%, and 15%) and the height of window opening floors (4 floors) on the indoor environment. The results show that when windows are opened on different floors, the window opening floor height (WOFH) of the upwind building has little influence on the downwind building, and similarly, the WOFH of the latter does not significantly affect the former. However, as windows are opened on the same floor with the same window opening percentage (WOP), the indoor ventilation rate of the upwind building increases with the increase of the WOFHs, but decreases slightly on the top floor (4th floor). In contrast, the indoor ventilation rate of the downwind building is not affected. Both upwind and downwind buildings experience an increase in ventilation rate with the increase of WOPs. Additionally, the ventilation rates of upwind and downwind buildings are linearly correlated with the ventilation ratios approaching 2. The findings of this study could provide a solid foundation for further study of the dispersion of pollutants in enclosed buildings.

Keywords: natural ventilation, cross ventilation, numerical simulation, enclosed building, wind tunnel experiment, window opening percentage

1 Introduction

Ventilation in buildings has increasingly garnered attention for its role in mitigating the transmission of infectious diseases and reducing the risk of Sick Building Syndrome through the provision of fresh air [1-3]. Building ventilation systems comprise both natural and mechanical ventilation methods. In comparison, natural ventilation excels in delivering a greater volume of fresh air and improving indoor environmental quality, all without incurring extra energy costs, which is particularly important in low-carbon buildings [4,5]. Different strategies of natural ventilation include cross-ventilation, single-sided ventilation, and stack ventilation [6]. Cross ventilation has historically been

H. Bilgin et al. (eds.), *Proceedings of the 2023 5th International Conference on Civil Engineering, Environment Resources and Energy Materials (CCESEM 2023)*, Advances in Engineering Research 227,
https://doi.org/10.2991/978-94-6463-316-0_36

achieved by residents opening windows on both sides during the appropriate seasons. Numerous studies have investigated the effects of factors such as opening location and size on natural ventilation, primarily through the use of wind tunnel experiments and numerical simulations.

Experimental studies, such as wind tunnel experiments, are combined with advanced experimental methods based on particle image velocimetry to explore air velocity fields and provide experimental data for validating Computational Fluid Dynamics(CFD). Karava et al. [7] indicated that the position of openings significantly affects both the airflow velocity and pattern within and through a building. Their findings showed that buildings with openings located in the lower section experience lower airflow velocities compared to those in the middle or upper section. Tominaga and Blocken's research [8] aligned with these results, showing that openings situated at the upper portion of the building exhibit the highest measured airflow velocities. Furthermore, their experiment highlighted that when windows are opened in a central position, there is an interaction between the air jet and the surrounding airflow in the room, resulting in the most effective removal of indoor pollutants.

Numerical studies on natural ventilation flows are usually performed using CFD, since these airflows in buildings with openings are considered challenging and the actual building geometries are more complex. Most studies gradually focus on the influence of various window characteristics (size, quantity, location, etc.) on natural ventilation in isolated, determinant, and staggered buildings. Considering the window opening position, Yang et al. [9,10] utilized numerical simulation techniques to investigate the impact of WOP (the proportion of window opening area relative to the external wall area on the window side) and various building layouts (determinant and staggered) on street canyon air quality. Their findings revealed that WOP primarily influences the pressure distribution around downwind buildings, leading to increased ventilation volumes in these structures as WOP increases. Furthermore, there was a significant decrease in pollutant concentration with increasing WOP (ranging from WOP = 0% to WOP = 10%), with this decrease being more pronounced in staggered buildings compared to determinant ones. Considering the impact of upwind buildings' occlusion, Fu Linli et al. [11] underscored the higher reliability of the Reynolds-averaged model in simulating occlusion when windows were present compared to cases without windows.

In Southeast Asia, historical architectural practices involved living in enclosed courtyards. Today, this architectural layout is commonly employed in commercial plazas, residential buildings, and campus structures [12-14]. Given the frequent use of such spaces by people, researchers have focused on studying airflow and air quality in both indoor and outdoor environments within enclosed buildings. Zhang Ningbo [12] utilized numerical simulation to investigate the impact of the entrance height on the airflow surrounding enclosed buildings. The results indicated that reducing the opening height on the windward side of the courtyard has a minimal effect on the courtyard space below 2 meters. Wang Yanling [13] employed numerical simulation to explore the impact of the number of openings in enclosed office buildings. The study found that in an enclosed layout, the wind speed is highest at the openings on the windward side, followed by the central measuring point within the enclosed space.

For enclosed buildings, the above studies have given a better understanding of the impact of building openings on the airflow characteristics in the courtyard but do not consider the indoor domain. Therefore, investigating the impact of WOPs and WOFHs on the coupling effect of the indoor and outdoor environments of enclosed buildings is considered in the present study. This paper selected an enclosed building as the numerical modeling and reliability verification model. It aims to investigate the influence of WOPs and WOFHs of enclosed buildings on the ventilation effect of upwind and downwind buildings and their interaction through flow rates, airflow velocity, and streamline characteristics.

2 Computational models and conditions

2.1 Physical Model

Figure 1 shows the schematic diagram of the model including the indoor and outdoor environments. Combined with the actual layout of the university buildings, a four-storey enclosed building is selected as the research object. Four windows are evenly distributed on the windward and leeward sides of the classroom. The vertical central section of one of the windows is taken as the analysis object (A-A section), as shown in Figure 1.

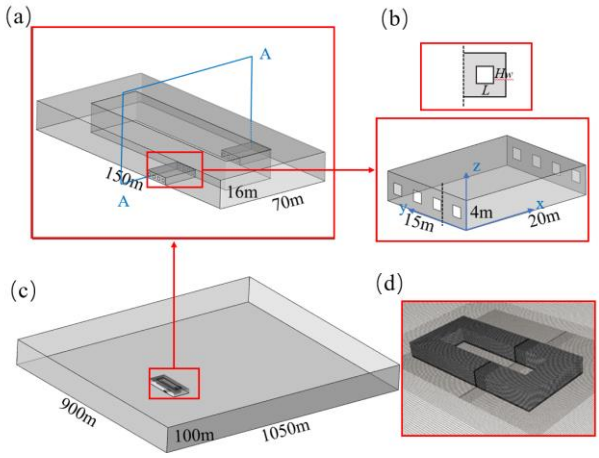

Fig. 1. Computational model: (a) building model, (b) classroom model, (c) computational domain, (d) mesh

The calculation area is set according to the recommended value in the existing studies [15,16], as shown in Figure 1(c). The finite volume method was used to discretize the governing equations and the second-order upwind scheme was used to discretize the governing equations [17]. The total number of grids is about 2.9×10^6, and the basic grid diagram is shown in Figure 1(d). The entrance of the computational domain is set

as the velocity inlet, and the velocity contour is described by the function relation with the roughness of the ground.

The vertical characteristics of wind speed are represented by a power exponential law [18,19] $U_z/U_h=(z/h)^{\alpha}$, and the turbulence intensity at z height I_z, $I_z=0.1(z/h)^{(-\alpha-0.05)}$, the turbulent kinetic energy k_z, $k_z=(I_zU_z)^2$ and turbulence dissipation rate ε_z, $\varepsilon_z=C_\mu^{1/2}k_z(U_h/h)\alpha(z/h)^{(\alpha-1)}$. z is any height, m; U_z is the average wind speed at this height, m/s; α is the ground roughness index. According to literature [15], α = 0.25 is taken here, the reference height h=10m and the standard reference wind speed at U_h=3.4m/s are defined here, C_μ is the empirical constant which equals 0.09. The outlet of the computing domain is set as the pressure outlet boundary condition, and the surface of building and ground adopt a non-slip wall. Symmetric boundary conditions are set for the remaining surface.

2.2 Mathematical Model

In the three-dimensional numerical calculation, according to the characteristics of practical problems, the indoor and outdoor fluid flow of a building can be simplified to a three-dimensional, steady and incompressible air flow, and the governing equation of the fluid can be written:

Continuity Equation:

$$\frac{\partial}{\partial x_j}\left(\rho u_j\right)=0 \tag{1}$$

Momentum Equation

$$\frac{\partial}{\partial x_j}\left[\rho u_i u_j-\left(\mu+\mu_{\mathrm{t}}\right)\frac{\partial u_i}{\partial x_j}\right]=-\frac{\partial p}{\partial x_j} \tag{2}$$

Using RNG k-ε turbulence model [20], the governing equations of turbulent kinetic energy and its dissipation rate can be written as follows:

$$\frac{\partial}{\partial x_j}(\rho u_j k-a_k\mu_{\mathrm{eff}}\frac{\partial k}{\partial x_j})=G_k+\rho k \tag{3}$$

$$\frac{\partial}{\partial x_j}(\rho u_j \varepsilon-a_\varepsilon\mu_{\mathrm{eff}}\frac{\partial \varepsilon}{\partial x_j})=C_{1\varepsilon}G_k\frac{\varepsilon}{k}+C_{2\varepsilon}\rho\frac{\varepsilon^2}{k} \tag{4}$$

where x_i is the component of Cartesian coordinates, u_i is the component in the direction of average velocity i. ρ is the air density; p is the average pressure; and μ and μ_t are the molecular viscosity coefficients of fluid and turbulent viscosity coefficients, respectively. k is the turbulent kinetic energy, μ_{eff} is the effective turbulent kinematic viscosity, G_k is the turbulent kinetic energy generated due to the gas velocity gradient, ε is the dissipation rate of the turbulent kinetic energy, the constant [21] $\alpha_k=\alpha_\varepsilon$ =1.39, $C_{1\varepsilon}$ = 1.42, $C_{2\varepsilon}$ = 2.

2.3 The rationality verification of numerical calculation method

To verify the reliability of the numerical model established in this paper, the experimental model of Kosutova et al. [22] was selected to simulate and reproduce the experiment with the numerical model established in this paper, and the results are shown in Figure 2.

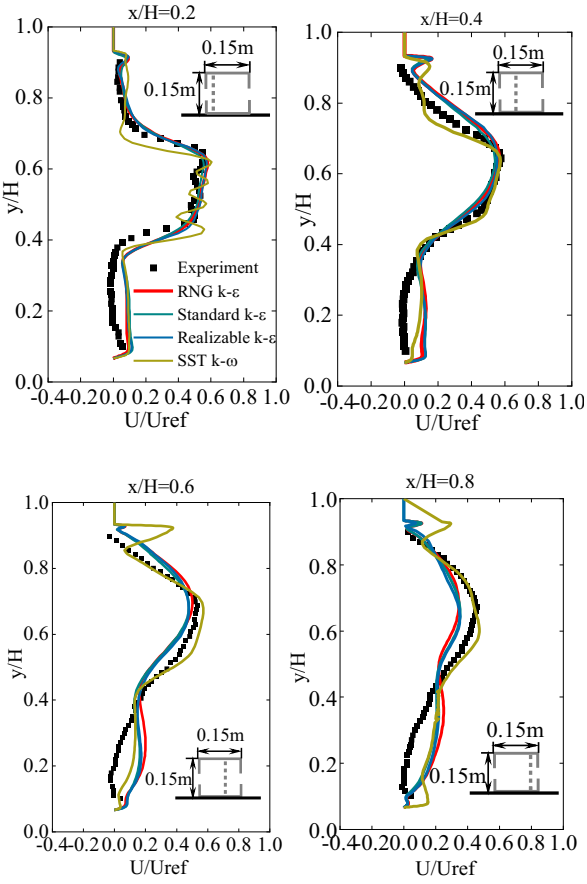

Fig. 2. Comparison of simulated dimensionless mean velocity results with experimental data

Figure 2 shows the variation curve of the dimensionless average velocity along the height direction at different positions of the building ($x/H = 0.2, 0.4, 0.6, 0.8$), where H is the height of the building. Figure 2 shows that the RNG k-ε turbulence model is in good agreement with the experimental data in most regions, especially in the central window region. Considering the calculation time cost and accuracy requirements, the RNG k-ε turbulence model is adopted for numerical calculation in this paper.

3 Simulation results and discussion

3.1 Effect of opening on different floors on ventilation

To investigate the mutual influence of WOFHs on the ventilation between the upwind-building (U) and downwind-building (D) with the same WOP(WOP=5%), we conducted 5 simulations when windows of the downwind building opened on the same floor (D1, the first floor) and windows of the upwind building opened on different floors (U0, all windows closed; U1, the first floor; U2, the second floor; U3, the third floor; U4, the fourth floor), respectively. In addition, 5 conditions were simulated when windows of the upwind building opened on the same floor (U1, the first floor) and windows of the downwind building opened on different floors (D0, all windows closed; D1, the first floor; D2, the second floor; D3, the third floor; D4, the fourth floor), respectively. Under a total of 10 simulation models, the indoor ventilation rate of the upwind building and the downwind building changes, as shown in Figure 3.

Figure 3(a) shows the influence of WOFH of upwind building on ventilation effect of downwind building at 5% WOPs. With the increase of WOFH of upwind building, the indoor ventilation rate of downwind building is less than 3%, which is basically unchanged. Figure 3(b) explores the influence of WOFH of the downwind building on the indoor ventilation effect of the upwind building. Compared with the downwind building without window openings (D0), when windows open on the first floor (U1D1), the indoor ventilation rate of the upwind building is significantly reduced, indicating that the opening of windows in the downwind building will have an impact on the ventilation effect of the upwind building. With the increase of WOFH of the downwind building, the reduction in the difference between the ventilation rate of the upwind building and that of the downwind building when windows are closed in the downwind building, presents a diminishing influence of the downwind building on the ventilation of the upwind building.

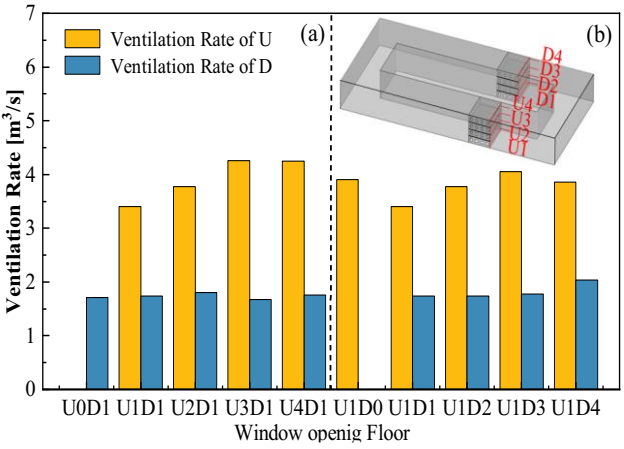

Fig. 3. Ventilation rate of the upwind building and the downwind building (WOP=5%)

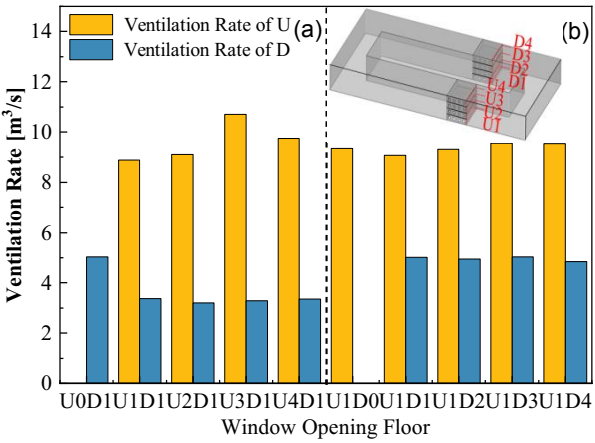

Fig. 4. Ventilation rate of the upwind building and the downwind building (WOP=10%)

Figure 4 illustrates the change of the indoor ventilation rate of the upwind building and the downwind building when the WOP is 10% and consistent with the prior conditions regarding WOFH. In total, there are 10 simulated models. Figure 4(a) reveals the variations in the WOFH of the upwind building do not significantly affect the indoor ventilation rate of the downwind building. However, with closed windows in the upwind building, it becomes evident that the presence of window opening in the upwind building has a significant impact on the indoor ventilation of the downwind building. Figure 4(b) demonstrates that changes of WOFH of the downwind building have a slight influence on the indoor ventilation rate of the upwind building, with a trend consistent with that observed when WOP is 5%.

With the increase of WOP, the impact of the upwind building on the ventilation of the downwind building becomes apparent. Specifically, with WOP=10%, the window openings in the upwind building decrease the indoor ventilation rate of the downwind building, while the WOFH shows no effect on this relationship. when the WOP becomes 10%, the upwind building's window opening reduces the indoor ventilation rate of the downwind building, but the WOFHs have no effect on it. The influence of the downwind building on the indoor ventilation of the upwind building exhibits a consistent pattern.

Figure 5 and Figure 6 depict the reciprocal effects of the upwind building and downwind building when WOFHs change with the same WOP(WOP=5%). With the increase of the WOFH in the upwind building, the position of the central vortex in enclosed buildings tends to move upward, resulting in an expanded influence range of vortex diameter and increased flow attachment on the leeward side of the upwind building. Compared with the downwind building with closed windows(U1D0), when windows open on the first floor of the downwind building (U1D1), the wind speed at the entrance of the windward side of the downwind building significantly decreases. However, the wind speed at the entrance gradually rises with the increase in the WOFH of the downwind building.

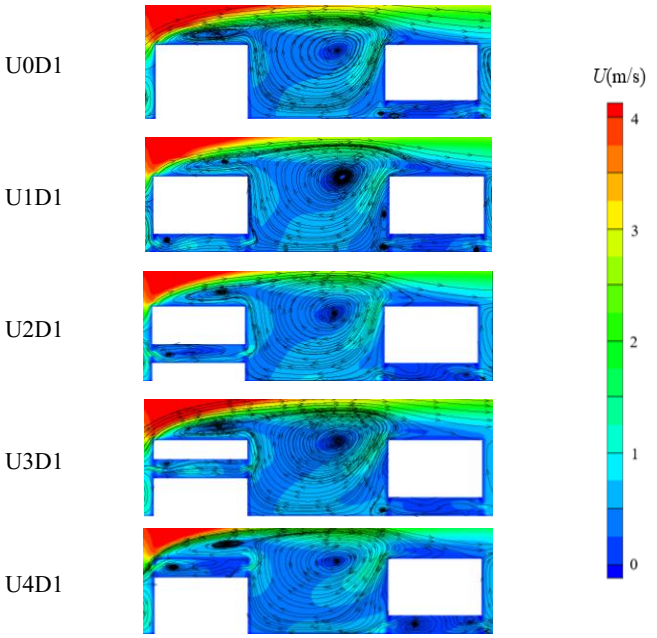

Fig. 5. Velocity contours and streamlines on plane A-A with different WOFHs of the upwind building

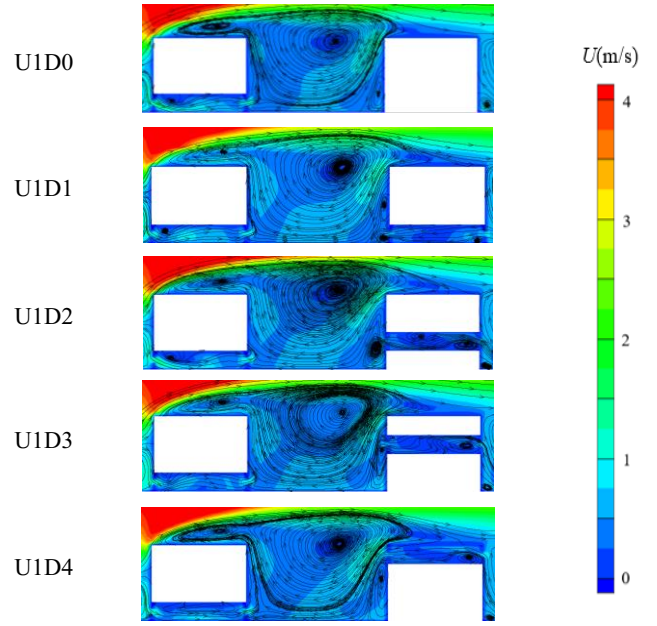

Fig. 6. Velocity contours and streamlines on plane A-A with different WOFHs of the downwind building

In general, the ventilation rate experiences a change of more than 10% only when windows are opened on the same floor, while for other cases, the change remains less than 5%. It indicates that different WOFHs have minimal impact on the ventilation effect of the enclosed building, while the window openings on the same floor have a greater impact. Therefore, the following is a further detailed study of the impact of the WOFH and WOP on the ventilation effect when windows are opened on the same floor.

3.2 Effect of window opening on the same floor on ventilation

Figure 7 shows the change in ventilation rate between the upwind building and the downwind building. In total, there are 8 simulation models, including window openings on the first floor(U1D1), window openings on the second floor(U2D2), window openings on the third floor(U3D3), and window openings on the fourth floor(U4D4), each at two WOPs(5% and 10%).

The results presented in Figure 7 reveal a general upward trend in the ventilation rate of the upwind building. However, a slight decrease in ventilation rate is observed for the fourth floor with window openings, primarily due to the influence of the vortex near the top floor. In contrast, the ventilation rate of the downwind building remains relatively stable, with changes staying within the 5% range, which can be regarded as negligible. Consequently, an increase in the WOFHs on the same floor leads to a significant enhancement in the indoor ventilation rate of the upwind building, while exerting minimal impact on the ventilation rate of the downwind building.

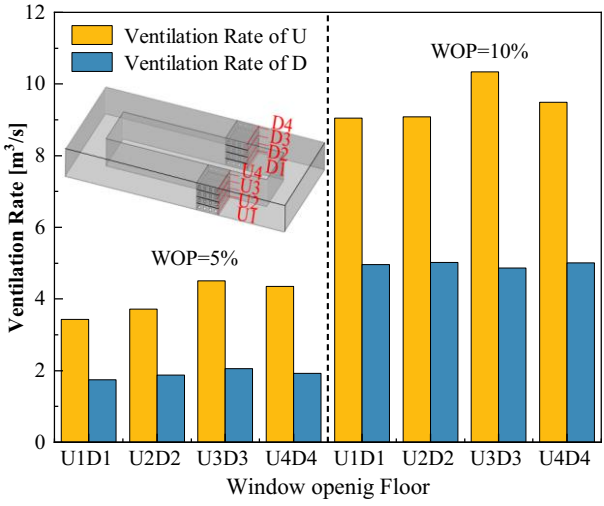

Fig. 7. Ventilation rate of the upwind building and the downwind building with window openings on the same floor of different WOFHs

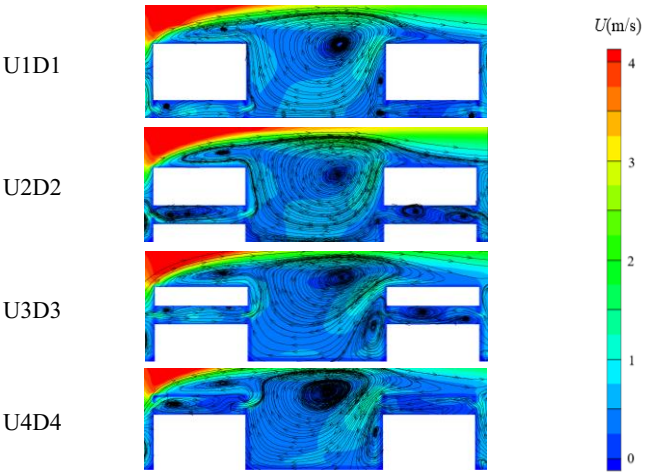

Fig. 8. Velocity contours and streamlines on plane A-A with window openings on the same floor

Figure 8 illustrates the airflow velocity and streamline distribution of the A-A profile at different WOFHs when the WOP of the upwind and downwind buildings is 5% on the same floor. The results indicate that with the increase of the WOFHs, the vortex at the center of the courtyard tends to move upward, and the scope of the vortex diameter decreases significantly. At the same time, the downwind building forms a small vortex at the bottom of the windward side, which may easily cause pollutants to accumulate here.

3.3 Effect of different WOPs on the same floor on ventilation

Investigating the impact of varying WOPs (5%, 7.5%, 10%, 12.5%, 15%) under similar conditions, this study conducted simulations for a total of 20 scenarios. These scenarios involved five different WOPs on four different floors (first floor, second floor, third floor, and fourth floor), respectively. The simulation results are presented in Figure 9.

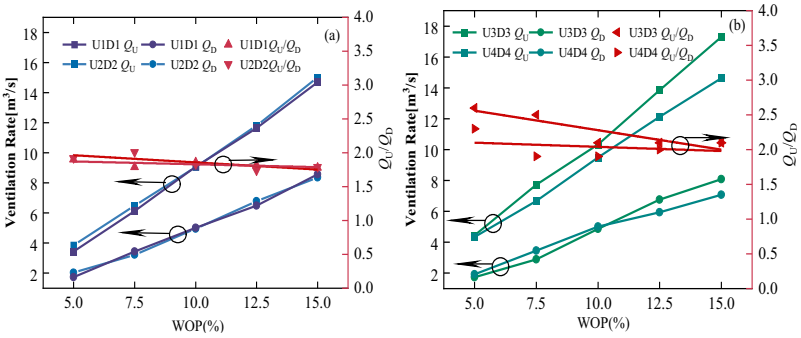

Fig. 9. Ventilation rate and the ventilation rate ratio of different WOPs with window openings on the same floor of four different WOFHs respectively

Figure 9(a) shows the impact of varying WOPs on the ventilation rates for the first and second floors. Similarly, Figure 9(b) illustrates how different WOPs affect the ventilation rates for the third and fourth floors. The results indicate a consistent trend that as the WOP increases, the ventilation rates for both upwind and downwind buildings show a steady and linear growth. Additionally, the ratio of ventilation rates between the upwind and downwind buildings maintains a linear relationship when window openings are on the same floor. While it shows a slight decrease as WOP increases. Notably, the ventilation rate within the upwind building with window openings on the third floor is significantly higher than that on other floors. This discrepancy can be attributed to the third floor's position at the airflow stagnation point [23], where the air pressure is higher compared to other locations, resulting in a more substantial ventilation rate through this specific position.

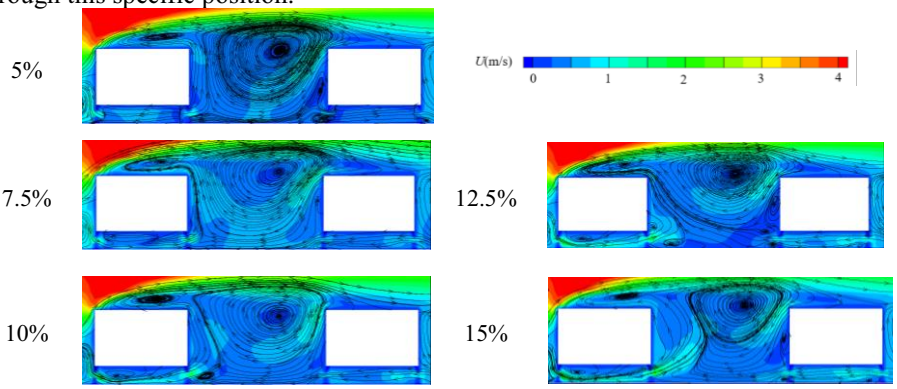

Fig. 10. Velocity contours and streamlines on plane A-A with five different WOPs

Figure 10 shows the airflow velocity and streamline distribution in section A-A with different WOPs when windows are opened on the first floor of the enclosed building. The results suggest that when windows are opened on the same floor, the vortex in the center of the courtyard tends to shift upward and the vortex diameter decreases with the increase of WOPs The airflow velocity increases at the opening of the leeward side of the upwind building, and the attached flow is blown away from the wall, which strengthens the airflow flow.

4 Conclusion

This study presents CFD simulations of cross-ventilation in an enclosed building. Through analyzing the influence of different WOPs and WOFHs on the ventilation effect of enclosed buildings, the following conclusions can be drawn from this study:

(1) As window openings of the upwind and downwind buildings are located on different floors, the impact of the WOFHs of either building's windows on the other building ventilation effect can be neglected, in contrast to situations where the window openings of both buildings are on the same floor.

(2) When the window openings of both buildings are on the same floor, whether the upwind and downwind buildings open the window or not has a significant influence on each other's ventilation effect. As the WOP increases, the effect of the window opening of the upwind building on the ventilation of downwind building becomes strong, while the window opening of the downwind building has the opposite effect on the ventilation of the upwind building.

(3) As window openings with the constant WOP are on the same floor, the increase of WOFHs results in a significant enhancement in the indoor ventilation rate of the upwind building, while the indoor ventilation rate of the downwind building is basically unchanged. As the increases of WOP on the same floor, both buildings experience a substantial increase in the indoor ventilation rates and the ratio of the ventilation rate of two buildings approaches 2.

Acknowledgments

This work was supported by the National Natural Science Foundation of China (Grant No. 42075179), and the Shanghai Ocean University Startup Fund for Young Scholars (Grant No. A2-2006-22-20031).

References

1. Jiang Z, Kobayashi T., Yamanaka T and Sandberg M. (2023). A literature review of cross ventilation in buildings. *Energy Build*. 113143.
2. Zhong H Y, Sun Y, Shang J, Qian F P, Zhao F Y, Kikumoto H, Bescos C J and Liu X C. (2022) Single-sided natural ventilation in buildings: a critical literature review. *Build Environ*, 212:108797.
3. Pan W, Liu S, Wang Y, Cheng X, Zhang H and Long Z. (2019) Measurement of cross-ventilation rate in urban multi-zone dwellings. *Build Environ*, 158:1-16.
4. Saadatjoo P, Badamchizadeh P and Mahdavinejad M. (2023) Towards the new generation of courtyard buildings as a healthy living concept for post-pandemic era. *Sustain. Cities Soc*. 104726.
5. Bhagat R K, Wykes M S D, Dalziel S B and Linden P F. (2020) Effects of ventilation on the indoor spread of COVID-19. *J Fluid Mech*. 903: F1.
6. Jiang Z, Kobayashi T, Yamanaka T and Sandberg M. (2023) A literature review of cross ventilation in buildings. *Energy Build*. 113143.
7. Karava P, Stathopoulos T and Athienitis A K. (2011) Airflow assessment in cross-ventilated buildings with operable façade elements. *Build Environ*. 46(1): 266-279.
8. Tominaga Y and Blocken B. (2016) Wind tunnel analysis of flow and dispersion in cross-ventilated isolated buildings: Impact of opening positions. *J. Wind. Eng. Ind. Aerodyn.* 155: 74-88.
9. Yang F, Kang Y, Gao Y and Zhong K. (2015) Numerical simulations of the effect of outdoor pollutants on indoor air quality of buildings next to a street canyon. *Build Environ*. 87: 10-22.
10. Yang F, Gao Y, Zhong K and Kang Y M. (2016) Impacts of cross-ventilation on the air quality in street canyons with different building arrangements. *Build Environ*. 104: 1-12.

11. Fu L L, Yin W, Wang T W and Zhang G. (2020) Effect of the porosity the upstream building on the natural ventilation of the downstream building and the reliability of its computational fluid dynamics simulation. *J. Civ. Environ. Eng*. 43(01): 229-242.
12. Zhang N B. (2014) Study on the air environment characteristics of the indoor and outdoor space of enclosed buildings. *Donghua University*.
13. Wang Y L. (2020) Research on the impact of enclosed office building layout on wind environment in Hangzhou. *Zhejiang University*.
14. Yang L, Liu X, Qian F and Niu S. (2020) Research on the wind environment and air quality of parallel courtyards in a university campus. *Sustain. Cities Soc*. 56: 102019.
15. Tominaga Y, Mochida A, Yoshie R, Kataoka H, Nozu T, Yoshikawa M and Shirasawa T. (2008) AIJ guidelines for practical applications of CFD to pedestrian wind environment around buildings. *J. Wind. Eng. Ind. Aerodyn*. 96: 1749-1761.
16. Mochida A, Tominaga Y, Murakami S, Yoshie R, Ishihara T and Ooka R. (2002) Comparison of various k-ε model and DSM applied to flow around a high-rise building-report on AIJ cooperative project for CFD prediction of wind environment. *Wind and Structures*. 5(2-4): 227-244.
17. Lee I, Lee S, Kim G, Sung J, Sung Y and Yoon Y. (2005) PIV verification of greenhouse ventilation air flows to evaluate CFD accuracy. *Transactions of the ASAE*. 48(6): 2277-2288.
18. Mei S J, Luo Z, Zhao F Y and Wang H Q. (2019). Street canyon ventilation and airborne pollutant dispersion: 2-D versus 3-D CFD simulations. *Sustain. Cities Soc.* 50: 101700.
19. Shirzadi M and Tominaga Y. (2022) CFD evaluation of mean and turbulent wind characteristics around a high-rise building affected by its surroundings. *Build Environ*. 225: 109637.
20. Snyder W H. (1994) Some observations of the influence of stratification on diffusion in building wakes. Stably stratified flows: flow and dispersion over topography. *Clarendon Press*. UK. 52: 301-324.
21. Yakhot V and Smith L M. (1992) The renormalization group, the ε-expansion and derivation of turbulence models. *J Sci Comput*. 7(1): 35-61.
22. Kosutova K, Van Hooff T, Vanderwel C, Blocken B and Hensen J. (2019) Cross-ventilation in a generic isolated building equipped with louvers: Wind-tunnel experiments and CFD simulation. *Build Environ*. 154: 263-280.
23. Erell E, Pearlmutter D and Williamson T. (2012) Urban microclimate: designing the spaces between buildings. *Routledge*, London.